Nonvolcanic Deep Tremor Associated with Subduction in Southwest Japan

Kazushige Obara

Deep long-period tremors were recognized and located in a nonvolcanic region in southwest Japan. Epicenters of the tremors were distributed along the strike of the subducting Philippine Sea plate over a length of 600 kilometers. The depth of the tremors averaged about 30 kilometers, near the Mohorovic discontinuity. Each tremor lasted for at most a few weeks. The location of the tremors within the subduction zone indicates that the tremors may have been caused by fluid generated by dehydration processes from the slab.

Long-period events and tremors with typical periods in the range of 0.2 to 2 s are often observed at active volcanoes and reflect the internal dynamics of the volcanic system (*1*). A possible tremor-generating mechanism is flow-induced oscillation in channels transporting magmatic fluid (*2*). We have identified and studied anomalous long-period tremors from a nonvolcanic area in southwest Japan by using the National Research Institute for Earth Science and Disaster Prevention's (NIED) high-sensitivity seismograph network (Hi-net), which is composed of about 600 stations installed throughout Japan to detect microearthquakes (*3*). The densely distributed high-sensitivity seismic stations provide a high-level detection capability for microearthquakes and offer us an opportunity to find and investigate very small amplitude tremors. Because the amplitudes of these tremors are very small, it is difficult to identify them with a single station or a sparse network.

National Research Institute for Earth Science and Disaster Prevention, Tenno-dai 3-1, Tsukuba, Ibaraki, 305-0006, Japan. E-mail: obara@bosai.go.jp

We observed small-amplitude tremors that lasted from a few minutes to a few days, as shown in fig. S1A. The tremors were observed simultaneously at several Hi-net stations, which indicates that they are not related to artificial noise. The predominant frequency of the tremors ranged from 1 to 10 Hz and was lower than that of ordinary earthquakes of similar size (10 to 20 Hz). We transferred the raw seismogram to root-mean-square (rms) amplitude for the filtered output (fig. S1B), and tremors were clearly seen for time windows of 35 to 50 min. The envelope shapes of the tremors were very similar at different stations. The envelopes had gradual rise times and differed from those of a normal earthquake, which has a spike-like envelope shape. The similar envelope amplitude pattern seemed to have been propagated with a velocity of 4 km/s, which we roughly estimated from paste-up traces plotted with the increasing epicentral distance. This means that the source of the tremors was located at a deep portion and the envelopes were propagated not by *P*-wave, but by *S*-wave velocity. Because it was very difficult to identify the initial *P*- and *S*-wave onset for the hypocentral determination, we applied a cross-correlation technique to get the distribution of the relative arrival time of the envelope (*4*). The spatial distribution of the

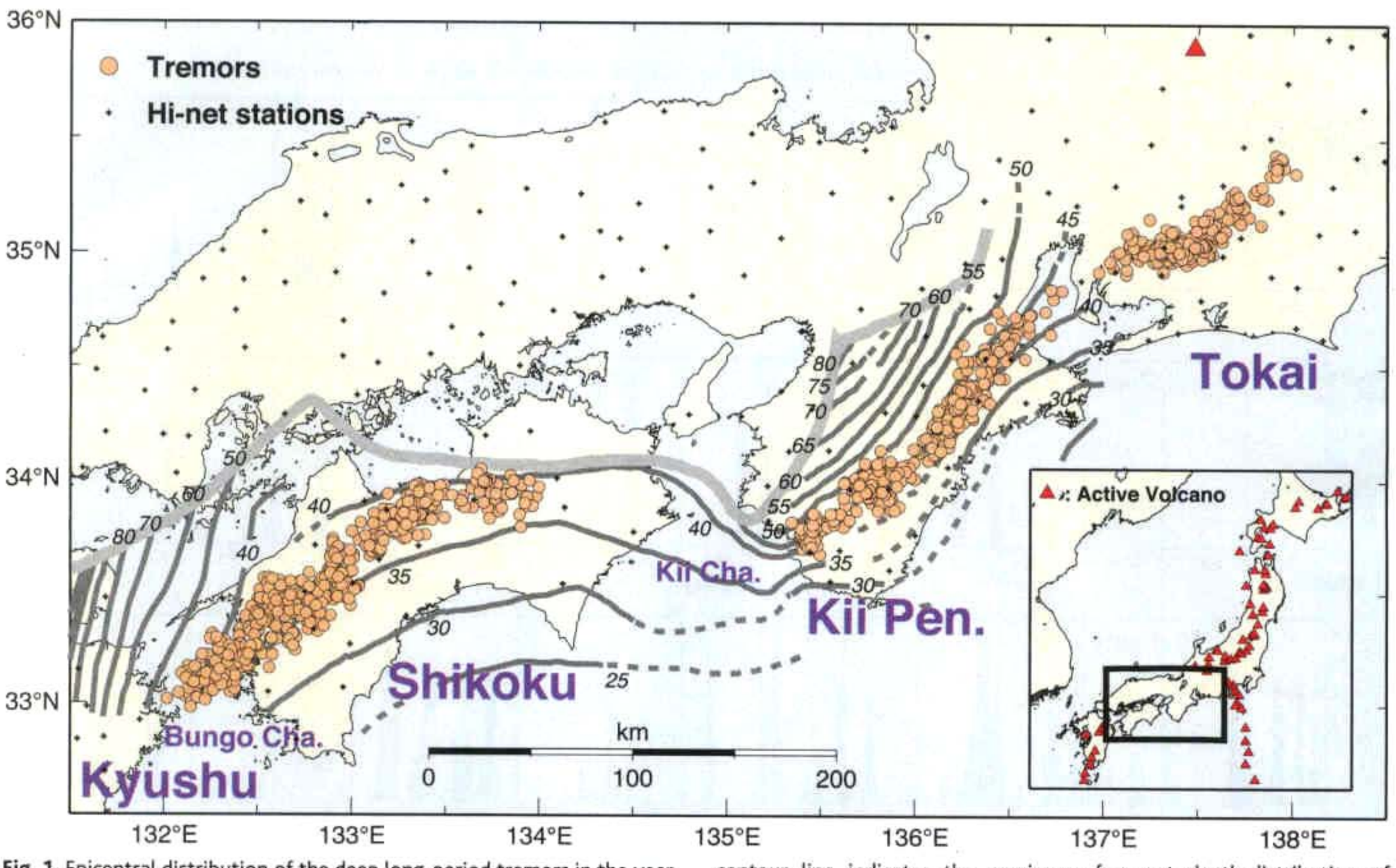

Fig. 1. Epicentral distribution of the deep long-period tremors in the year of 2001. The circle indicates the center of epicenters of tremors calculated every hour. The crosses represent the Hi-net stations. The depth contour line indicates the maximum frequent depth-distribution of earthquakes inside the subducting Philippine Sea plate, and the gray line represents the leading edge of the subducting Philippine Sea plate (*11*).

arrival time was used to determine the hypocenter of the tremor using a depth-dependent layered *S* wave–velocity model, which was used for the local hypocentral determination. In this method, the hypocenter of the tremor was obtained once every 1 min, if the coherent envelope of the tremor continued. However, each hypocenter was sometimes scattered because of the lack of *P* wave–arrival time data and contamination of the envelope shape by occurrence of tremors in different areas at the same time. Therefore, the center of the distribution of tremors determined for 1 hour was plotted (Fig. 1) as the epicenter of the tremor in the time interval if the hypocenters were distributed within an area whose radius was 10 km. The tremors were distributed along the strike of the subducting Philippine Sea plate over a length of 600 km from the Tokai area to the Bungo channel, between Shikoku and Kyushu Island. The epicentral distribution of the tremors corresponded to the seismicity with the depth range from 35 to 40 km in the Shikoku area, and with the depth range from 40 to 45 km in the Kii peninsula. No tremor has been detected around the Kii channel between the Shikoku and the Kii peninsula, nor in the east part of the Shikoku. The well-estimated source depths of the tremors are concentrated at a depth of about 30 km, near the Mohorovic discontinuity.

We looked for the tremor activity in every 1-hour envelope seismogram and determined the frequency in units of 1-hour periods. The active period of most tremors generally continued for several days, and sometimes for a few weeks (Fig. 2). After an active period, the region was quiet for a few months. The tremors sometimes seemed to be triggered by a nearby relatively large earthquake. For instance, active tremor sequences started in the Tokai area from 10 April and 2 June, 2001, after M (local magnitude determined by Japan Meteorological Agency) 5–class earthquakes occurred at a location 40 to 50 km away from the tremor region, on 3 April and 1 June, respectively. The Geiyo earthquake (*M* 6.7) occurred on 24 March, and then a tremor became active in the Shikoku area. On the other hand, tremor activity sometimes finished right after a nearby earthquake. For example, in the Tokai area, tremor activity lasted for about 2 weeks in September and then stopped when the Western Aichi earthquake (*M* 4.1) occurred near the tremor.

The tremors did not always remain in one region in an episode but sometimes migrated (fig. S2). In the western Shikoku area, tremor activity started at the beginning of January at approximately 133.0°E and then moved gradually toward the west with a velocity of about 13 km/day. In the same area, the tremor activity in August moved from west to east with the same velocity as observed in January.

Deep long-period tremors often include impulsive body waves with a predominant frequency of about 1 to 2 Hz. Such an impulsive phase, which is thought to be an *S* wave, has been established by hypocentral determination to be a deep low-frequency microearthquake (*5*). Such a tremor might be a continuous sequence of low-frequency earthquakes. Such low-frequency earthquakes (long-period events), with a depth of around 30 km, occur not only around active volcanoes (*6*, *7*) but also near active fault systems (*8*), according to Hi-net. These low-frequency earthquakes are sometimes followed by tremor-like long wave trains, where each wave train has a duration of about several minutes to several hours. However, the tremors observed in southwest Japan had a longer duration and a larger source area than did the low-frequency earthquakes.

Considering the long duration and mobility of the tremor activity, the generation of tremors may be related to the movement of fluid in the subduction zone. The subducting slab may liberate aqueous fluid by dehydration. Therefore, large amounts of fluid may be generated in the slab and move to the slab surface or the depth of the Mohorovic discontinuity. At high temperature and pressure, aqueous fluid mixed with silicate melts exists as a supercritical fluid (*9*). The presence of supercritical fluid may reduce the friction and

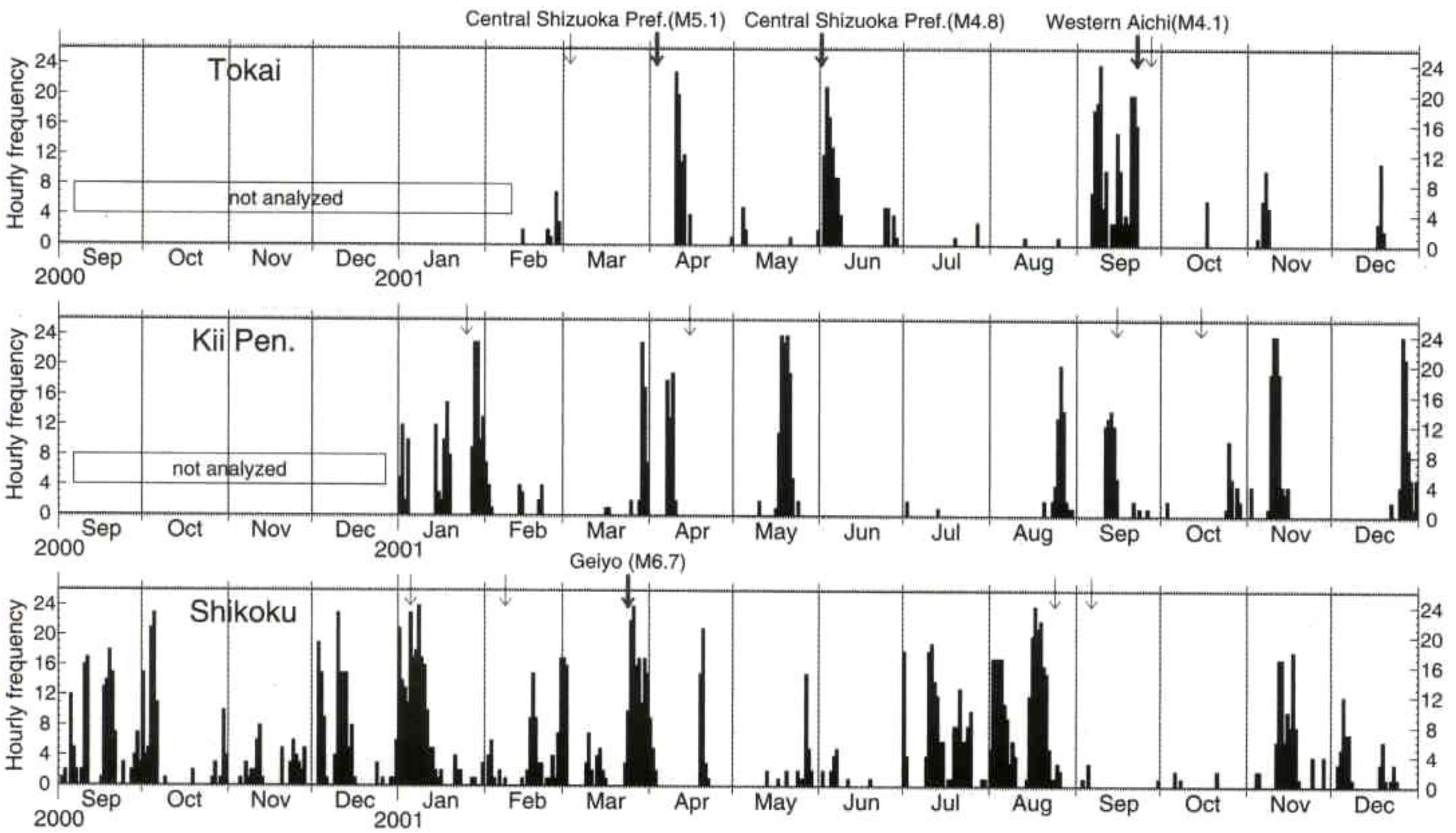

Fig. 2. Time sequence of the tremor activity in the Tokai, the Kii peninsula, and the Shikoku area. The frequency in units of 1-hour periods in which the tremor was recognized is plotted. The arrows indicate major earthquakes greater than *M* 4, which occurred near the tremor active zone. The arrows attached with the name of the earthquake indicate relatively large earthquakes, which might have affected the tremor activity.

change the fracture criterion of the rock by increasing the pore pressure and/or create new cracks through hydraulic fracturing. Therefore, tremor activity with a long duration time might be caused by a chain reaction of small fractures caused by the supercritical fluid. If the condition of the tremor generation is unstable, the additional supply of fluid to an almost saturated system, or stimulation by nearby earthquake shaking, might be able to trigger the observed tremor.

References and Notes

1. B. Chouet, *Nature* **380**, 309 (1996).
2. B. R. Julian, *J. Geophys. Res.* **99**, 11859 (1994).
3. NIED Hi-net is a newly established seismic network (*10*). Each station consists of a three-component velocity seismometer with a natural frequency of 1 Hz installed at the bottom of a borehole with a depth of 100 to 200 m. The data are digitized at each station with a sampling frequency of 100 Hz, and then the data packets attached with the absolute time information from a Global Positioning System clock are transmitted to the data center.
4. Vertical-component waveforms for a pair of stations are converted to envelopes with a frequency range of higher than 4 Hz and with a smoothing time of 10 s, and they are resampled with a sampling interval of 1 s. A pair of envelope seismograms with a length of 2 min is used for calculation of the cross-correlation coefficient by moving a trace with the time lag of every 1 s to another fixed reference trace. The time lag, which gives the maximum correlation coefficient, should be the difference of the arrival time for a coherent seismic signal in the selected 2 min observed in the two stations. If the maximum correlation coefficient is less than 0.9, the time lag is not applied for the further process because there is no coherent signal. Such a correlation process is carried out for all pairs of stations in the target area. The measured time lags with a good correlation are averaged spatially to calculate the distribution of the relative arrival time like the net adjustment, which is used in the geodetic survey. The cross-correlation analysis is carried out with the moving time window of 1 min; therefore, we can calculate the location of tremors once every 1 min, continuously.
5. A. Katsumata, N. Kamaya, *Seismol. Soc. Jpn. Fall Meeting* B16 (2001).
6. M. Ukawa, K. Obara, *Bull. Volcanol. Soc. Jpn.* **38**, 187 (1993).
7. A. Hasegawa, A. Yamamoto, *Tectonophysics* **233**, 233 (1994).
8. S. Ohmi, *Eos* **82** (fall suppl.), 871 (2001).
9. H. Bureayu, H. Keppler, *Earth Planet. Sci. Lett.* **165**, 187 (1999).
10. K. Obara *et al.*, *Eos* **81** (fall suppl.), 863 (2000).
11. M. Nakamura *et al.*, *Ann. Disaster Prev. Res. Inst. Kyoto* **40 B-1**, 1 (1997).

30 January 2002; accepted 11 April 2002

Microscopic View of Structural Phase Transitions Induced by Shock Waves

Kai Kadau,[1,2]* Timothy C. Germann,[3] Peter S. Lomdahl,[1] Brad Lee Holian[1]

Multimillion-atom molecular-dynamics simulations are used to investigate the shock-induced phase transformation of solid iron. Above a critical shock strength, many small close-packed grains nucleate in the shock-compressed body-centered cubic crystal growing on a picosecond time scale to form larger, energetically favored grains. A split two-wave shock structure is observed immediately above this threshold, with an elastic precursor ahead of the lagging transformation wave. For even higher shock strengths, a single, overdriven wave is obtained. The dynamics and orientation of the developing close-packed grains depend on the shock strength and especially on the crystallographic shock direction. Orientational relations between the unshocked and shocked regions are similar to those found for the temperature-driven martensitic transformation in iron and its alloys.

Since the ancient Greeks, the structural transformation in steel has been used to harden swords by rapid cooling. The underlying physics was first seriously explored by Martens in the late 19th century, and, because of his work, the diffusionless structural phase transitions in steel and other materials have become known as martensitic transformations (*1*, *2*). Concomitant effects, such as the aforementioned hardening, pseudoelastic, and shape memory effects, are used to design special materials for medical and engineering applications (*1*, *2*). Structural transformations are also observed in biological systems, as some virus species use the pressure-induced martensitic transformation to infect bacteria cells (*3*).

Despite this great importance in technology and nature, many open questions remain, mostly related to the underlying atomistic processes. Martensitic transformations are characterized by a collective movement of atoms across distances that are typically smaller than one nearest-neighbor spacing. Crystallographic orientational relations between the two phases exist, and the resulting crystal exhibits fine-scale inhomogeneities such as slip, twinning, and stacking faults. The best known martensitic transformation is that of Fe and its alloys; for example, Fe/Ni alloys transform on cooling from a high-temperature face-centered cubic (fcc) phase to a low-temperature body-centered cubic (bcc) phase. Other examples are alloys based on CuAl, NiTi, NiAl, and ceramics like ZrO_2 (*2*), to name only a few. All these transformations are first order, which means they exhibit hysteresis and can be overheated or undercooled like the fluid-solid transition of water. The temperature and the height of the energy barrier between the two phases determine whether the transformation is induced by thermal fluctuations (homogeneous nucleation) or by preexisting defects, which locally reduce the energy barrier and act as nucleation centers (heterogeneous nucleation).

Such structural transformations can be caused by either temperature or pressure changes. Shock waves lead to increases in both pressure and temperature, inducing a close-packed structure due to a martensitic-like transformation (*4*, *5*). Ab initio electronic structure calculations (*6*) and molecular-dynamics simulations (*7*) are appropriate methods for atomic-scale investigations of these phenomena. Whereas ab initio methods are limited to very small system sizes, large-scale molecular-dynamics (MD) simulations using empirical potentials give insight into the motion of millions of atoms on the pico- and nanosecond time scale for a variety of physical problems, including crack propagation (*8*, *9*), friction (*10–12*), dislocation dynamics (*13*, *14*), shock waves (*15*, *16*), and structural phase transitions (*17–21*).

Here, we report the investigation of shock-induced structural phase transitions using massively parallel MD simulations (*22*). Simulations were carried out for two different embedded-atom method (EAM) potentials (*23*) describing the forces between the atoms in a metal (*24*). Shock waves were initiated by a "momentum mirror" (*15*), which specularly reflects any atoms reaching the face of a perfectly flat, infinitely massive piston moving at the piston (or particle) velocity u_p (*25*). The resulting shock wave moves in front of the piston at the shock velocity u_s. To minimize surface and edge effects, periodic boundary conditions perpendicular to the shock direction are applied, simulating a pseudoinfinite lateral dimension. Shock waves were generated in both the [001] and [011] directions of an initially perfect bcc

[1]Theoretical Division, Los Alamos National Laboratory, Los Alamos, NM 87545, USA. [2]Theoretische Tieftemperaturphysik, Gerhard-Mercator-Universität Duisburg, Lotharstraße 1, 47048 Duisburg, Germany. [3]Applied Physics Division, Los Alamos National Laboratory, Los Alamos, NM 87545, USA.

*To whom correspondence should be addressed: E-mail: kkadau@lanl.gov